OPEN ACCESS

University of BRISTOL

Valenzuela Gutierrez, A., Reid, J. P., Bzdek, B. R., & Orr-ewing, A. J. (2018). Accuracy Required in Measurements of Refractive Index and Hygroscopic Response to Reduce Uncertainties in Estimates of Aerosol Radiative Forcing Efficiency. *Journal of Geophysical Research: Atmospheres*, *123*(12), 6469-6486. https://doi.org/10.1029/2018JD028365

Publisher's PDF, also known as Version of record

Link to published version (if available):
10.1029/2018JD028365

Link to publication record in Explore Bristol Research
PDF-document

This is the final published version of the article (version of record). It first appeared online via AGU at https://agupubs.onlinelibrary.wiley.com/doi/abs/10.1029/2018JD028365 . Please refer to any applicable terms of use of the publisher.

University of Bristol - Explore Bristol Research
General rights

This document is made available in accordance with publisher policies. Please cite only the published version using the reference above. Full terms of use are available:
http://www.bristol.ac.uk/red/research-policy/pure/user-guides/ebr-terms/

Journal of Geophysical Research: Atmospheres

RESEARCH ARTICLE
10.1029/2018JD028365

Accuracy Required in Measurements of Refractive Index and Hygroscopic Response to Reduce Uncertainties in Estimates of Aerosol Radiative Forcing Efficiency

Antonio Valenzuela[1], **Jonathan P. Reid**[1], **Bryan R. Bzdek**[1], **and Andrew J. Orr-Ewing**[1]

[1]School of Chemistry, University of Bristol, Bristol, UK

Key Points:
- More precise data set of refractive indices for nonabsorbing aerosol than previously used in other studies are retrieved from BB-CRDS
- It is possible to provide more accurate RFE values using refined optical and microphysical properties from CRDS measurements
- The first time the sensitivity of the radiative forcing efficiency to uncertainties in the complex refractive index and the hygroscopic response is evaluated

Correspondence to:
A. Valenzuela,
av16946@bristol.ac.uk

Citation:
Valenzuela, A., Reid, J. P., Bzdek, B. R., & Orr-Ewing, A. J. (2018). Accuracy required in measurements of refractive index and hygroscopic response to reduce uncertainties in estimates of aerosol radiative forcing efficiency. *Journal of Geophysical Research: Atmospheres*, *123*. https://doi.org/10.1029/2018JD028365

Received 22 JAN 2018
Accepted 11 MAY 2018
Accepted article online 18 MAY 2018

©2018. American Geophysical Union. All Rights Reserved.

Abstract The magnitude of aerosol radiative forcing resulting from the scattering and absorption of radiation is still uncertain. Sources of uncertainty include the physical and optical properties of aerosol, reflected in uncertainties in real and imaginary refractive indices (n and k) and relative humidity (RH). The effect of RH on the geometrical size of aerosol particles is often reported as a hygroscopic kappa parameter (κ). The objective of this study is to explore the sensitivity of radiative forcing efficiency (RFE) to changes in particle properties in order to better define the accuracy with which optical and hygroscopic measurements must be made to reduce uncertainties in RFE. Parameterizations of precise values of n and k are considered as functions of RH for ammonium sulfate (AS) and brown carbon (BrC). The range of the RFE estimated for typical uncertainties of n and κ for AS of 0.1 μm dry radius is less than ±7% and is not affected by an increase of RH. For typical sizes of AS in the atmosphere (0.35 μm dry radius), the range of the RFE increases to ±20% at 90% RH and ±15% at 99% RH. Absorbing small BrC particles (0.1 μm dry radius) cause cooling at the top of the atmosphere, and as RH and κ increase, the RFE is more negative compared to the usual assumptions of dry unhygroscopic BrC. For larger BrC particles (0.35 μm dry radius), the change in RFE for RHs ~100% compared to dry conditions can take values around −100%.

1. Introduction

Direct radiative forcing (RF) caused by anthropogenic aerosols is one of the major contributors to changes in the radiative balance of the Earth-atmosphere system (Adams et al., 2001; Nemesure et al., 1995). In clear-sky conditions aerosols scatter solar radiation back to space, reducing solar irradiance at the ground. This effect is usually known as "the aerosol direct effect" (Boucher & Lohmann, 1995). Through the scattering and absorption of solar radiation, the direct effect is one of the largest uncertainties in RF (Intergovernmental Panel on Climate Change, 2013). Using 16 models, Myhre et al. (2013) simulated the RF of the aerosol direct effect from total anthropogenic aerosols and found a wide range of values from −0.58 to −0.02 W/m^2, with a mean of −0.27 W/m^2. Clearly, more effort is required to reduce the uncertainty of the RF associated with the aerosol direct effect.

The parameter that governs how light interacts with an aerosol particle is the extinction cross section (σ_{ext}), which depends on the complex refractive index (m), the radius of the particle (r), and the wavelength of the radiation. The real part (n) of the complex refractive index impacts on scattering radiative processes and the imaginary part (k) of the complex refractive index impacts on absorbing radiative processes. n is a fundamental optical parameter that influences light-scattering coefficients, such as scattering cross section (σ_{sp}), backscattering cross section (σ_{bsp}), single scattering albedo (ω), and the asymmetry parameter (g). The asymmetry parameter is defined as the intensity-weighted average cosine of the scattering angle:

$$g = \frac{1}{2}\int_0^{\pi} \cos\theta \cdot P(\theta) \cdot \sin\theta \cdot d\theta \quad (1)$$

where θ is the angle between incident light and scattering direction and $P(\theta)$ is the angular distribution of scattered light (the phase function). The values of g range between −1 for entirely backscattered light and +1 for entirely forward scattered light (Boucher, 1998). The determination of n and k can be very challenging because of the mixed composition of aerosol in the atmosphere, their dynamic change through chemical processing and change in mixing state, and the hygroscopic response of particles as the ambient relative humidity (RH) varies. In addition, the solid-aqueous particle phase transition affects the size and the shape of the particle. Not only does this have implications for the aerosol properties (Wang et al., 2008), but departures from sphericity make the determination of n and k challenging.

Precise characterization of the RH dependence of n and k is essential for use in radiative transfer codes and climate models. However, the chemical complexity of aerosol particles in the atmosphere demands new analytical and experimental approaches capable of improving our understanding of the chemical and physical processes affecting the aerosol properties. As an example, cavity ring down spectroscopy (CRDS) is one well-established technique to retrieve the extinction properties of aerosol (Miles et al., 2011). A typical measurement by CRDS involves an ensemble of particles with a known size distribution, composition, and concentration. The particles are passed into an optical cavity in order to measure the effective extinction cross section, σ_{ext} (Mason et al., 2012). By fitting measurements of σ_{ext} for different particle sizes with Mie theory, selected from a polydisperse distribution of particle sizes, it is possible to determine precise values of n. However, this approach has significant sources of error, which arise due to uncertainties in quantification of the particle number concentration and the inherent polydispersity of even a nominally monodisperse ensemble of particles (Miles et al., 2011). Typical uncertainties can be at the level of ±2%.

A significant advance over ensemble CRDS is the single-particle CRDS. This new experimental approach allows retrieval of accurate σ_{ext} values, made on a single aerosol particle, the size of which is monitored over an extensive period of time as it responds to changes in RH. To achieve such measurements, a combination of a Bessel laser beam trap and cavity ring down spectrometer (BB-CRDS) has been used to retrieve accurate σ_{ext} values for a single particle of well-defined composition (Cotterell, Mason, et al., 2015; Cotterell, Preston, et al., 2015; Cotterell et al., 2016; Mason et al., 2015; Walker et al., 2013; Willoughby et al., 2017). The extinction efficiency for a single particle, Q_{ext}, is

$$Q_{ext} = \frac{\sigma_{ext}}{\sigma_{geo}} \tag{2}$$

where σ_{geo} is the geometric cross section for a spherical particle with radius, r, inferred independently from the angularly scattered light profile. A camera coupled to a 20× microscope objective situated orthogonal to the direction of illumination was used to collect the angular variation in the elastically scattered light, referred to as the phase function ($P(\theta)$), with the central scattering angle at θ = 90°. For the objective used with NA = 0.42 and an angular range collected of 49.7°, the angular variation in scattering intensity covered the range between 65.2° and 114.9° with a resolution of 0.05° per camera pixel. Due to objective aberrations this angle range was reduced to 44.8°. This procedure has been described previously (Cotterell, Preston, et al., 2015; Cotterell et al., 2017). We have shown that the value of the RH-dependent n can be retrieved with an accuracy better than ±0.01% from these single-particle BB-CRDS measurements for coarse mode droplets containing atmospherically relevant inorganic solutes, provided the measurement can be made with continuous variation in the particle size as the RH is varied (Cotterell, Preston, et al., 2015). For fine mode droplets, an accuracy of better than ±0.2% is typical. A detailed explanation of the BB-CRDS technique and the theory underlying single-particle measurements can be found in recent papers (Cotterell, Mason, et al., 2015; Cotterell, Preston, et al., 2015; Cotterell et al., 2016; Mason et al., 2015; Walker et al., 2013; Willoughby et al., 2017). Given this improved level of accuracy in optical constant measurements, it is appropriate to consider how this could translate into reductions in uncertainties in RF.

To isolate sources of uncertainty in direct RF, such as the influence of uncertainty in optical constants for aerosol, it is common to represent the forcing normalized to the aerosol loading, or the direct radiative forcing efficiency (RFE). RFE at the top of the atmosphere can be used to assess the effect over the incoming radiation of a thin aerosol layer placed at the lower troposphere. As RFE is not dependent on the aerosol load, it is possible to evaluate the cooling or warming of the atmosphere as well as the sensitivity of RFE as a function of the intrinsic physical and optical properties of the aerosol (r, ω, and g). In fact, many studies have used this quantity to explore uncertainties in optical constants and the ensuing sensitivities in RF (Dinar et al., 2008; Erlick et al., 2011; Zarzana et al., 2014).

The precision with which n is known has an impact on the precision of the RFE. Zarzana et al. (2014) reported that an uncertainty of less than 1% in RFE requires an error in n below 0.003 for nonabsorbing AS. More significantly, an uncertainty ±0.01 in the k value translates into an uncertainty in the forcing of roughly ±20% for absorbing BrC aerosol particles of radius between 75 and 100 nm. However, the single most important parameter in determining direct aerosol forcing is the RH. Pilinis et al. (1995) established that an increase of the RH from 40 to 80% resulted in an increase of the RF by a factor of 2.1. In fact, part of the overall uncertainty in

sulfate aerosol RF is related to the increase in the scattering radiation as a function of RH and the fraction of the scattered radiation into the upward hemisphere (β; Charlson et al., 1992; Colberg et al., 2003; Li et al., 2001; Penner et al., 1994). These quantities depend on the particle size and the wavelength; it is well known that particle size is a strong function of RH (Garland, 1969; Tang & Munkelwitz, 1994; Tang et al., 1997). Several parameterizations to represent the dependence of particle size on RH have been proposed (Duplissy et al., 2011; Good et al., 2010; Kreidenweis et al., 2005; Petters & Kreidenweis, 2007; Titos et al., 2016). Thus, the microphysical and optical properties of aerosol must both be scaled with variation in RH. There are a few studies that account for the variation in aerosol optical properties with the RH and the impact on RFE (Kiehl et al., 2000; Li et al., 2001). The value of n used in these studies was retrieved from volume-weighted averages of refractive indices of the solute and water. Erlick et al. (2011) reported that the differences arising from using the conventional volume mixing rule and empirically derived refractive indices may be significant when investigating regional aerosol forcing.

Using the approach described above for nonabsorbing aerosols, this paper will assess the accuracy with which the value of n, κ, and the dependence on RH must be determined in order to better constrain the RF of aerosols. Later, we will examine the sensitivity of RFE to the RH dependence of both n and k for absorbing aerosol using a parameterization proposal by Hänel (1976). To explore these two cases, scattering and scattering with absorption, we have chosen to focus on two anthropogenic aerosol species that exert the strongest magnitudes of RF on the climate system.

As a benchmark case for scattering particles, we consider the well-known sulfate aerosol, which is a water-soluble inorganic species. For such hygroscopic particles, the size and the composition are strongly affected by changes in ambient RH, leading to changes in n and r (Cotterell et al., 2017). In the troposphere, ammonium sulfate ($(NH_4)_2SO_4$) and ammonium bisulfate (NH_4HSO_4) are the dominant sulfate containing compounds (Charlson et al., 1978; Nemesure et al., 1995). They exist as dry particles at low RH and undergo abrupt uptake of water at the deliquescence RH (Pilinis et al., 1995). In this analysis, we only consider the dry sulfate component as dry ammonium sulfate (AS): several studies have shown that the direct forcing is relatively insensitive to whether the aerosols consist of mixtures of the two aerosol components previously mentioned (Haywood et al., 1997; Nemesure et al., 1995; Pilinis et al., 1995).

As an example of an aerosol that both absorbs and scatters light, we consider brown carbon (BrC) aerosol. Several authors have considered BrC as a model of absorbing aerosol, but a wide range of n and k values for BrC may be found in the literature. k for BrC at or near to 532 nm wavelength ranges from 0.05 given by Zarzana et al. (2014) to a value of 0.003 reported by Chen and Bond (2010). In addition, the precision which these values are reported is unclear. Additionally, these values are retrieved in dry conditions, even though it can be expected that ambient conditions affect the k values through changes with RH, affecting the values of RF. Therefore, a better understanding of the limitations of n and k retrieval methods is needed.

Although the parameterizations themselves contribute errors (Myhre et al., 2004), these errors are much smaller than uncertainties in aerosol properties. Cotterell et al. (2017) quantified the overall agreement between Cauchy parameterization for n_{fit} (RH) and the measured and literature values n_j (RH) for different salts by evaluating the mean difference in n, where

$$\left|\overline{\Delta n}\right| = \frac{1}{J}\sum_{j=1}^{J}\left|n_{\text{fit}} - n_j\right| \tag{3}$$

in which the summation is over all j measured-literature values. In the worst of the cases studied the difference was at most 0.0044.

Aerosol optical properties calculated with Mie theory using accurate parameters are the inputs to estimate the RFE as a function of the RH in the visible spectrum and for the most atmospherically relevant size ranges. A sensitivity study is performed to establish the accuracy required in determinations of n, k, and in hygroscopic kappa parameter, κ, to improve predictions of RFEs. Our objective is to explore the level of accuracy required in measurements of these parameters to achieve a desired level of accuracy in the estimation of the RFE.

2. Parameterizations of Optical Constants and Hygroscopic Growth

2.1. Dependence of Particle Size on the Relative Humidity

Many studies of the hygroscopic growth of aerosol particles as a function of the ambient RH can be found in the literature (D'Almeida et al., 1991; Duplissy et al., 2011; Fitzgerald, 1975; Good et al., 2010; Kreidenweis et al., 2005; Petters & Kreidenweis, 2007; Rovelli et al., 2016; Tang, 1996). The growth factor, G, is defined as the ratio of the aerosol particle radius r at a specified RH to the radius of the corresponding dry aerosol r_0. G depends on the chemical composition of the particle, but assuming a particle of fixed initial dry chemical composition, then the G will only depend on particle size and RH as

$$G(r_0, \mathrm{RH}) = \frac{r(\mathrm{RH})}{r_0} \tag{4}$$

To describe the aerosol water uptake in the warm moist atmosphere, a precise description of the equilibrium behavior of a liquid solution droplet with respect to the water content of its environment is necessary. Although the Köhler equation can be used, for convenience we use the approximate κ-Köhler model proposed by Petters and Kreidenweis (2007) to provide the relation between the particle radius, r, measured at different water activities (a_w) with the radius in dry conditions, r_0. For 100 nm particles and typical growth factors, this approximation generally leads to a 1–2% error in the water activity (Koehler et al., 2006):

$$r = r_0 \cdot \left(1 + \kappa \cdot \frac{a_w}{1 - a_w}\right)^{1/3} \tag{5}$$

where a_w is equivalent to RH (%)/100 when neglecting the Kelvin effect based on droplet size. If the influence of surface curvature is ignored, the a_w is equal to the saturation ratio or the ratio of the vapor pressure of water over the drop to the saturation vapor pressure of water at that temperature. This is justified in our case, because the Kelvin effect is small for large particles (diameter $>$ 100 nm), which are the most relevant to light scattering and absorption (Zieger et al., 2010). κ characterizes the hygroscopicity response of the solute. In this study, the κ value used for AS is that reported by Koehler et al. (2006).

2.2. Wavelength and Relative Humidity Dependence of the Real Refractive Index for Nonabsorbing Aerosols

The wavelength dependence of the n of many transparent and absorbing materials in the visible and near-infrared spectral ranges can be described by the well-known Sellmeier equation (Sellmeier, 1871):

$$n^2 = 1 + \sum_{i=1}^{N} \frac{B_i \lambda^2}{\lambda^2 - C_i} \tag{6}$$

where n is the refractive index at the wavelength λ and B and C are fitting coefficients. If $N = 3$, equation (6) is referred to as the three-term Sellmeier equation. Measurements of the n of the medium at six different wavelengths are required to calculate the six Sellmeier constants B_1, B_2, B_3, C_1, C_2, and C_3 and to approximate the dispersion curve. Least squares fitting routines have been widely applied to fit the three-term Sellmeier equation to a set of experimentally determined values of n (Sutton & Stavroudis, 1961; Tatian, 1964, 1984). In our study, the Sellmeier equation fit is based on our very recent single-particle measurements of aerosol optical properties (Cotterell et al., 2017).

If the wavelength range of the measurements is limited to the visible region, or a wider range with negligible absorption, the n for many materials can be represented by equation (6) with expansion to only $N = 1$ (Sutton & Stavroudis, 1961). Therefore, the final expression used is

$$n^2 = 1 + \frac{B\lambda^2}{\lambda^2 - C} \tag{7}$$

The B and C Sellmeier coefficients are calculated from the fits to the experimental data and are smooth functions of the RH, parameterized as quadratic polynomials in term of the a_w.

$$B = b_0 + b_1 \cdot (100 \cdot a_w) + b_2 \cdot (100 \cdot a_w)^2 \tag{8}$$

$$C = c_0 + c_1 \cdot (100 \cdot a_w) + c_2 \cdot (100 \cdot a_w)^2 \tag{9}$$

The parameters (b_0, b_1, b_2, c_0, c_1, and c_2) were determined by performing a least squares fit, minimizing the residual between the values determined from experimental phase function and extinction cross section from BB-CRDS measurements, optical tweezers data, bulk refractometer measurements, and literature data (n_{405}, n_{473}, n_{532}, n_{560}, n_{589}, and n_{633}) and the n generated by the Sellmeier equation (Cotterell et al., 2017).

2.3. Relative Humidity Dependence of the Complex Refractive Index for Absorbing Aerosols

The parameterization for n using only a Sellmeier equation expansion to $N = 1$ is valid only in the visible spectrum with negligible absorption, as discussed in the previous section. In our study, it has only been verified for nonabsorbing aerosols. Extending the use of this approach to the more challenging case of absorbing aerosols, where information about the imaginary component of the refractive index is needed, has not been verified, and we instead apply a more straightforward volume-weighted approach. In this sense, in order to determine how the values of n and k of absorbing aerosols affect RFE at different RHs, their variation with water content must be calculated. Given the large uncertainties associated with these values for BrC, we assume molar volume additivity, that is, that the refractive indices as a function of RH can be computed as volume-weighted averages of the refractive indices of the dry aerosol and water on the ultraviolet and visible parts of the spectrum according to the expression given by Erlick and Frederick (1998):

$$n = n_w + (n_0 - n_w)\left(\frac{r_0}{r}\right)^3 \tag{10}$$

$$k = k_w + (k_0 - k_w)\left(\frac{r_0}{r}\right)^3 \tag{11}$$

where n and k are the real and imaginary parts of the refractive index of the BrC aerosol at a specific RH. n_0 and k_0 are the real and imaginary parts of the refractive index of the BrC aerosol under dry conditions, and n_w and k_w are the real and imaginary parts of the refractive index of water. We also limit our calculations to a wavelength of 532 nm. Again, equation (5) is used to provide the relationship between the particle radius at an elevated RH, r, with the radius under dry conditions, r_0. Values from 1.63 to 1.67 for n and from 0 to 0.1 for k are considered under dry conditions for BrC (Dinar et al., 2008). We have considered the κ value for BrC provided by Taylor et al. (2017) for organic carbon aerosol ranging between 0.05 and 0.15. In order to evaluate the effect of the unhygroscopicity on n and k, and hence in RFE, the lower limiting value of κ was reduced to zero.

2.4. Aerosol Optical Properties as a Function of RH: Estimation of the Direct Radiative Forcing Efficiency

Although the shape of the particles is an important parameter influencing the optical properties and the direct climate forcing (Wang et al., 2008), we have assumed in our study that the particles are spherical and homogeneous in refractive index, applying Mie theory for ease of analysis. Considering the parameterizations for r and n as a function of RH and wavelength, the interaction of the light with a single particle can be calculated using Mie theory (McCartney, 1976; van de Hulst, 1957). The input parameters used to supply the Mie code were n, k, and the size parameter (x) calculated for spherical particles as

$$x = \frac{2 \cdot \pi \cdot r}{\lambda} \tag{12}$$

where r is the radius of the particle at the specific RH and λ is the wavelength of the radiation.

In our study, four aerosol radiative properties are calculated: Q_{ext}, ω, g, and backscattering fraction (β) including dependence on particle size, composition, RH, and wavelength. These optical parameters are necessary to estimate the RFE at the top of the atmosphere caused by a thin aerosol layer in the lower troposphere from the equation proposed by Haywood and Shine (1995). Some previous publications have reported the use of this treatment to study the RFE (Dinar et al., 2008; Erlick et al., 2011; Haywood & Boucher, 2000; Randles et al., 2004; Zarzana et al., 2014). Our calculations of RFE are derived using the same equations and base-level assumptions as those by Erlick et al. (2011).

$$\mathrm{RFE} = \frac{\Delta F}{\mathrm{AOD}} = \mathrm{SD}(1 - A_{\mathrm{cld}}){T_{\mathrm{atm}}}^2(1 - R_{\mathrm{sfc}})^2\left[2R_{sfc}\frac{1 - \varpi}{(1 - R_{\mathrm{sfc}})^2} - \beta\varpi\right] \tag{13}$$

where AOD is the aerosol optical depth, S is the solar constant (set to 1,370 W/m^2). For the rest of the parameters, we assume standard conditions a of a continental area. D is the fractional day length (set to 0.5), A_{cld} is

the fractional cloud cover (set to 0.61), T_{atm} is the solar atmospheric transmittance (set to 0.76), and R_{sfc} is the surface albedo (set to 0.15). The β is the average upscatter fraction (the fraction of scattered sunlight that is scattered into the upward hemisphere), which is a function of hemispheric backscatter fraction b, defined as the ratio of backscattering efficiency to total scattering efficiency and ϖ is the single scattering albedo caused of a uniform and optically thin aerosol layer. The parameter β is calculated from the Henyey–Greenstein phase function:

$$\beta = 0.082 + 1.85 \cdot b - 2.97 \cdot b^2 \tag{14}$$

whereas b is derived from g through the equation (Wiscombe & Grams, 1976):

$$b = \frac{1-g^2}{2g}\left(\frac{1}{\sqrt{1+g^2}} - \frac{1}{1+g}\right) \tag{15}$$

The relative sensitivity observed for the change in RFE relative to a reference value, ΔRFE, is presented as a percentage and calculated from the equation:

$$\Delta\mathrm{RFE} = \frac{\mathrm{RFE} - \mathrm{RFE}_{\mathrm{reference}}}{\mathrm{RFE}_{\mathrm{reference}}} \times 100 \tag{16}$$

2.5. Radiative Forcing Efficiency Dependency on RH, Wavelength and Particle Size

We first present some general characteristics observed in simulated Q_{ext} and g for purely scattering sulfate aerosol particles of a fixed dry particle size before considering in full the size dependence and the impact of absorption. These general characteristics are similar to those reported and described in numerous previous publications, although we more completely examine the dependence on wavelength based on our recent parameterization of n on RH and wavelength for AS. These simulations are useful for setting the context for the simulations that will be presented in section 3.

The dependencies of n and x on RH and wavelength for a dry particle of radius 0.1 μm are shown in Figures 1a and 1b, respectively. The value of n increases as RH decreases and as the wavelength becomes shorter: values below 1.4 occur when the RH is higher than 80%, increasing to values above 1.45 at RHs below 50% (Figure 1a). The values of n reported in our previous study at a wavelength of 532 nm are consistent with those reported by Flores et al. (2012) at 80% and 90% RHs for AS. Further, in our study, we extend the calculation of n to a wider range of RHs and wavelengths, which will enable us to reproduce the real environment conditions more completely. As can be seen in Figure 1b, counter to n, the value of x is largest at high RHs when hygroscopic growth is at its largest. At the shortest wavelengths, x increases by a factor of 1.3 at low RHs up to a factor of 1.8 at high RHs. This has well-known large implications for radiative effects depending on the size range of particles considered. Regarding the dependence of x with the wavelength, the smallest values for this parameter occur for higher wavelengths due to its inverse dependence with wavelength. Overall, the dependency of the RFE with particle size and RH is rather complicated as was pointed out by Pilinis et al. (1995). More detailed analysis can be found in section 3.

Calculations of Q_{ext} and g from Mie theory are shown in Figures 1c and 1d, respectively. Both parameters present a clear dependence on RH and wavelength. The impact of n but mainly of x on Q_{ext} values comes from changes to size and therefore the geometric cross section. Further, particles have higher Q_{ext} at high RH when x reaches the highest values. Although n shows lower values at high RHs, which would suggest that Q_{ext} would be reduced (smaller optical contrast compared to air), the stronger weight of x leads to larger values of Q_{ext} at high RHs. The extinction of light decreases with increase in wavelength, although this change is not obvious and depends on the RH. Overall, the values of Q_{ext} below 70% RH at all wavelengths are lower than 1.4; when RH ranges from 70% to 90%, Q_{ext} takes values in a wider range with a maximum around of 1.8 between wavelengths of 400 and 450 nm (Figure 1c). The g increases with RH at all wavelengths, with a sharper increase at wavelengths shorter than 500 nm (Figure 1d). The particles are more efficient at scattering radiation in the forward direction as they grow in size with increase in RH, as g takes values around 0.7. This parameter decreases as the wavelength increases due to the approach to the Rayleigh scattering limit with increasing wavelength.

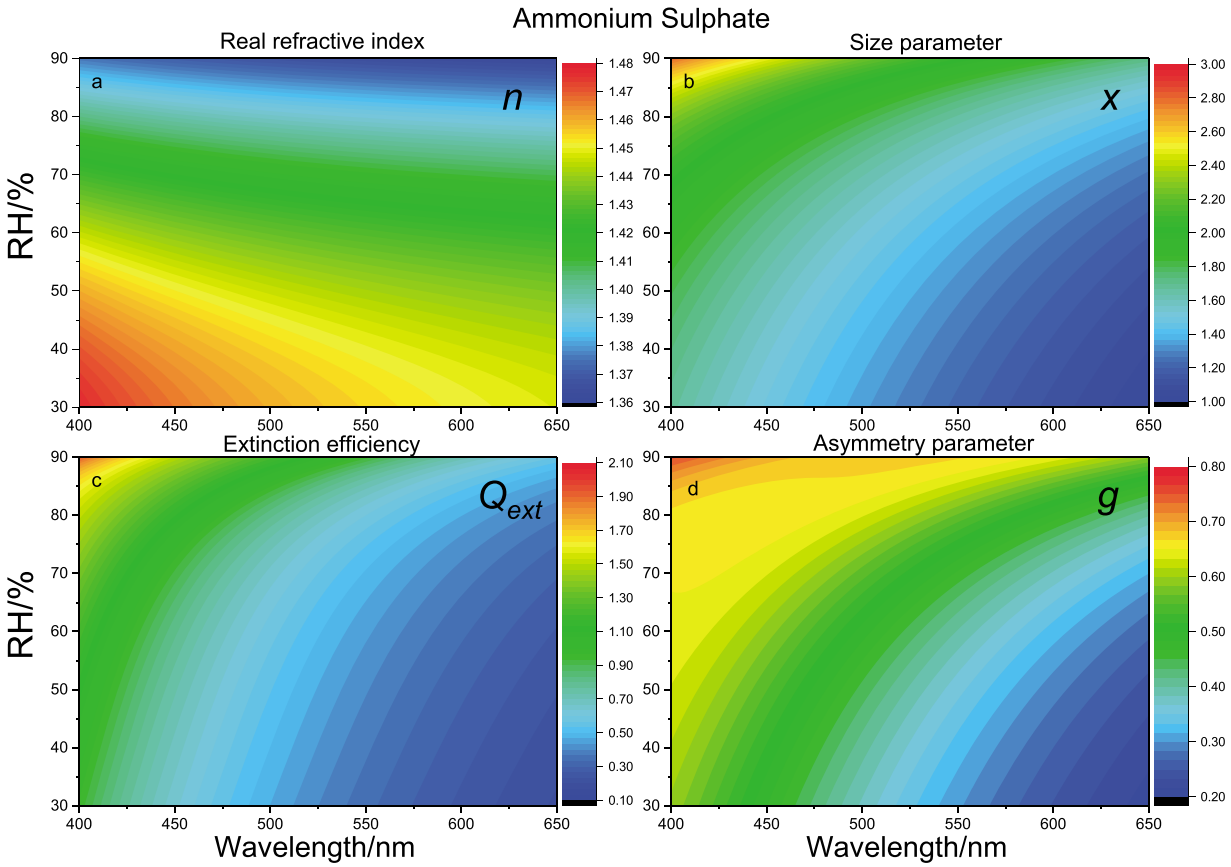

Figure 1. Contour plots representing the parameterization as function of both wavelength and RH for aqueous aerosol containing AS particles of (a) n, (b) x, (c) Q_{ext}, and (c) g. Note the different color scales in each part of the figure.

The RFE for dry particles of 0.1 and 0.35 μm radius are compared in Figures 2a and 2b, respectively. Particles of around 0.35 μm and smaller in the atmosphere have the largest climate impact (Heald et al., 2014; Wang et al., 2008). The RFE shows strong dependencies on RH and wavelength for particles of 0.1 μm radius with values from -28 to -22 W · m^{-2} · AOD^{-1} for RHs ranging between 60% and 90% and for the shortest wavelengths (Figure 2a). An increase in RH translates into less cooling at the top of the atmosphere by AS. More negative RFE values are achieved (-40 W · m^{-2} · AOD^{-1}) as RH decreases for wavelengths above 500 nm. The size of particles decreases, and g takes lower values leading to an increase in the radiation scattered in the backward direction into space.

As the size of the dry particles increases, the x is shifted to larger values, changing the extinction values in a nonmonotonic way due to the existence of resonance structures. Thus, the RFE varies nonmonotonically with RH and wavelength (Figure 2b). Overall, across the full range of RH and wavelengths, the RFE takes less negative values in comparison with smaller particles.

3. Results

Previous studies have examined the sensitivities of RFE to uncertainties in n and k (Erlick et al., 2011; Zarzana et al., 2014). Zarzana et al. (2014) focused their analysis on dry aerosol conditions, whereas Erlick et al. (2011) evaluated the RFE caused by aerosol at different RHs. To our knowledge, no previous studies have estimated the sensitivity of RFE to hygroscopic growth factor and optical constants, particularly for absorbing BrC aerosol. Our aim is to assess the level of instrumental accuracy required by measurements of the optical constants and hygroscopicity if a specific level of accuracy in the RFE is required. This will be informative for future instrumental development. To set this context, we first consider the levels of accuracy achieved by current techniques.

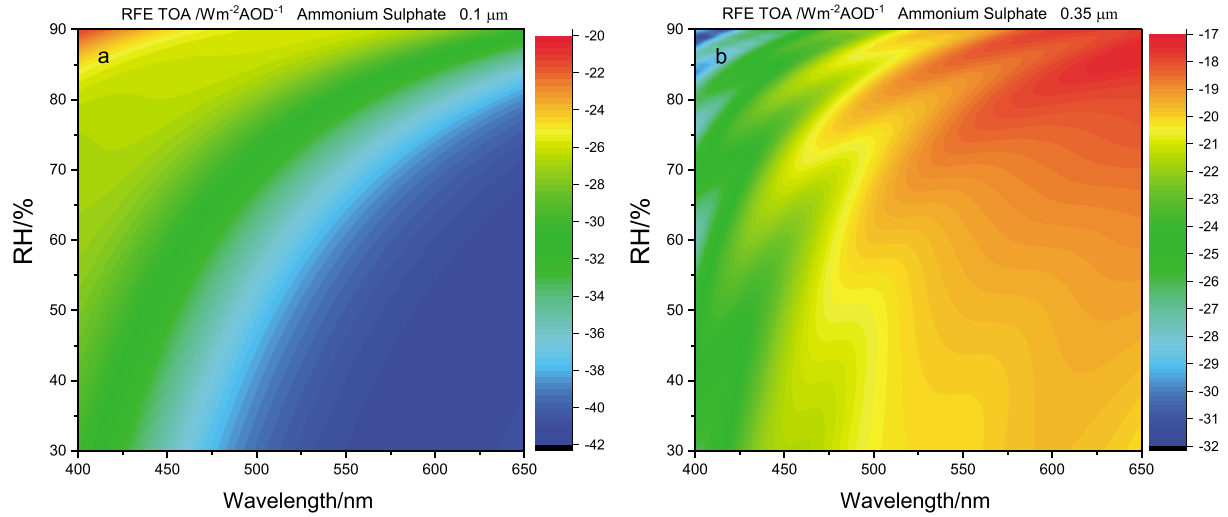

Figure 2. Contour plots representing the RFE as function of both wavelength and RH for aqueous aerosol containing AS particles of dry radius (a) 0.1 μm and (b) 0.35 μm.

3.1. Assessment of the Accuracy of Previous Measurements of Optical Constants and Aerosol Hygroscopicity

Mason et al. (2012) established that ensemble CRDS is unable to determine n with an accuracy of better than ~ ±0.02. More recent work by Zarzana et al. (2014) examined the uncertainty of measurements of n for non-absorbing AS aerosol over the range 1.42 to 1.62 and at fixed wavelength of 532 nm in dry conditions. When ensemble CRDS measurements are made at four AS particle diameters from 150 to 300 nm, they concluded that the retrieved values of n had an associated level of precision of ±0.015. These authors also estimated that an uncertainty in n of 0.003 leads to an uncertainty in RFE of 1%. However, the precision in n can be greatly improved when probing a single particle instead of ensemble CRDS measurements, with an accuracy reported of better than ±0.0007 from optical tweezer measurements (Mason et al., 2015). This level of accuracy is sufficient to assess the reliability of different mixing rules in representing the optical properties of aerosol (Cotterell, Mason, et al., 2015). Indeed, with respect to radiative effects, Erlick et al. (2011) estimated that the difference between the conventional volume mixing rule and empirically derived refractive indices may be an important one when investigating regional aerosol forcing.

When measuring the k of absorbing aerosols, Zarzana et al. (2014) demonstrated that a significant uncertainty in k values accompanied retrievals from ensemble CRDS measurements alone (uncertainty of ±0.03) from six particle diameters. They concluded that this uncertainty was considerably reduced by adding photoacoustic spectroscopy measurements of the same aerosol, particularly for mild/weakly absorbing aerosol such as BrC. For absorbing particles with $k > 0.6$, the uncertainty in k was of ±0.1, and for absorbing particles with $k < 0.3$, the uncertainty was around of ±0.01.

When determining the hygroscopic response of aerosol, Koehler et al. (2006) determined limiting values of κ of 0.33 and 0.72 from particle hygroscopicity measurements with a humidified tandem differential mobility analyzer (HTDMA) for AS aerosol. In recent paper, Rovelli et al. (2016) evaluated the accuracy of aerosol hygroscopic growth factor over a wide range in RH using a comparative kinetics cylindrical electrodynamic balance (CK-EDB) for different aerosols, a technique that can also be applied to secondary organic aerosol samples (Marsh et al., 2017). In the case of AS, the uncertainty in κ was reduced to ±0.01. On the other hand, using water soluble organic carbon, Taylor et al. (2017) estimated the hygroscopic growth at 90% RH reporting a κ value ranging from 0.05 to 0.15. An attempt to quantify the hygroscopic growth effects of organic aerosol over climate was addressed by Rastak et al. (2017). They studied the sensitivity of the Earth's radiative budget to assumptions about organic aerosol hygroscopicity and CCN activity, calculating the RF with κ values between 0.15 and 0.05 using two different climate models, namely, the atmospheric module of NorESM (Kirkevåg et al., 2013) and ECHAM6-HAM2 (Zhang et al., 2012). NorESM simulated a global average difference of about -1.02 W/m^2 in aerosol radiative effects between cases with κ values of 0.15 and 0.05 for water soluble organic carbon. Therefore, the sensitivity of climate forcing to κ is substantial if

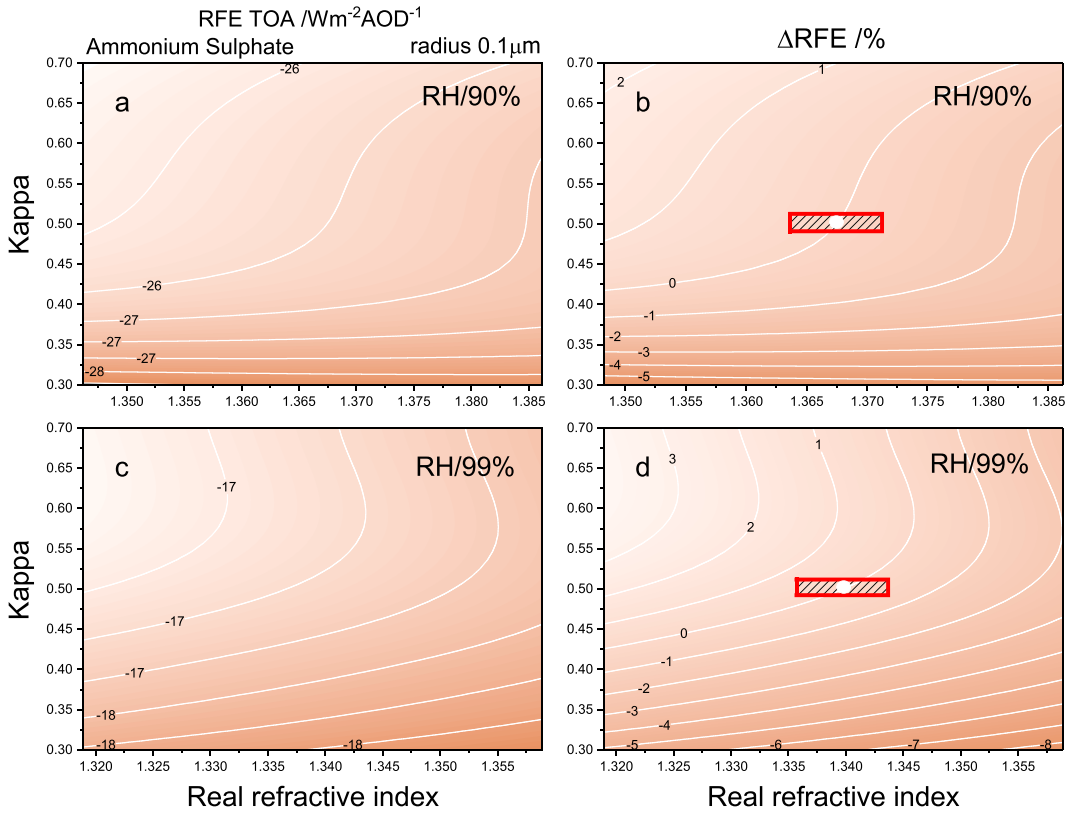

Figure 3. Contour plots representing (a) RFE and (b) ΔRFE as function of *n* and κ for AS particles of dry radius 0.1 μm at 532 nm wavelength and 90% RH (the white dot means reference value for *n* and κ). (c and d) Same as (a) and (b) but for 99% RH. The full ranges in *n* and κ represent the typical uncertainty ranges in these values from conventional approaches. The red boxes indicate typical uncertainties achieved by more refined measurements of *n* (±0.003) from BB-CRDS and measurements of κ (±0.15) using a comparative-kinetic EDB.

we consider that the climate forcing of anthropogenic aerosol particles during the industrial period is about −1 W/m^2 (Stocker et al., 2013).

To our knowledge, the coupling of uncertainties in complex refractive indices and the κ has not been addressed, particularly with a view to determining how accurate instruments must be. In addition, most previous analyses have considered only dry aerosol conditions and a single wavelength. The optical dispersion is not considered in *n* and *k* values.

3.2. Sensitivity of the RFE to Refractive Index and Hygroscopic κ-Factor for Nonabsorbing Aerosol

As far as we are aware, this study represents the first assessment to consider the combined uncertainties in hygroscopic growth, as reported by the κ and uncertainties in *n* in an estimate of the precision of the RFE for AS. We assume that the AS particles are spherical and consider two different dry particle radii (0.1 and 0.35 μm), presenting results for two different RH values (90 and 99%). The RFE is calculated from equation (13) at a wavelength of 532 nm for values of *n* and κ over their anticipated uncertainty ranges. The value of ΔRFE is calculated as the difference between the calculated RFE (equation (13)) at a chosen pair of values (*n* and κ) and RFE calculated from the reference case values of *n* and κ. The range of *n* values we have chosen is equivalent to the uncertainty range retrieved by Mason et al. (2012) from ensemble BB-CRDS measurements (±0.02). Regarding the κ value, the uncertainty range used is that provided by Koehler et al. (2006) for AS aerosol with κ values between 0.33 and 0.72. The pair of (κ, *n*) reference values are determined as follows: for κ we consider the mean value (0.52) and for *n* we consider the value obtained from equation (10) at the appropriate RH.

Figures 3a and 3b show the RFE and the ΔRFE, respectively, where ΔRFE is calculated relative to the reference case of *n* and κ (given by the white dot) at 90% RH and for a dry particle radius of 0.1 μm. The RFE is negative

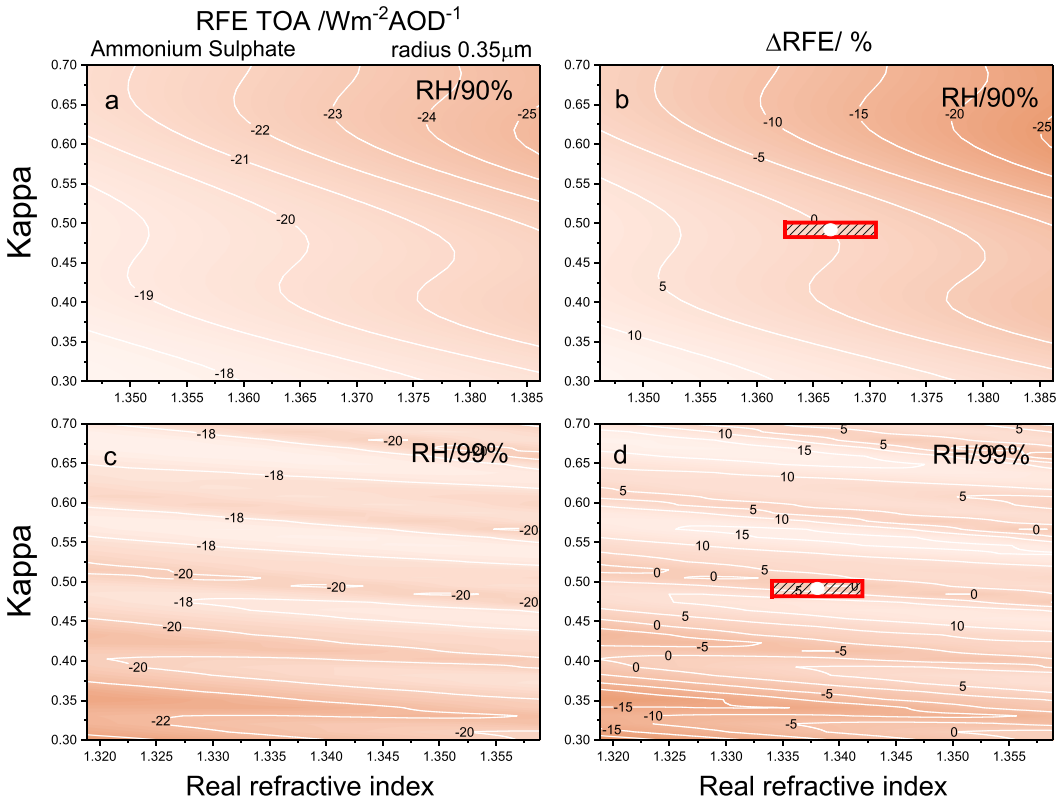

Figure 4. Contour plots representing (a) RFE and (b) ΔRFE as function of *n* and κ for AS particles of dry radius 0.35 μm at 532 nm wavelength and 90% RH (the white dot means reference value for *n* and κ). (c and d) Same as (a) and (b) but for 99% RH. The full ranges in *n* and κ represent the typical uncertainty ranges in these values from conventional approaches. The red boxes indicate typical uncertainties achieved by more refined measurements of *n* (±0.003) from BB-CRDS and measurements of κ (±0.15) using a comparative-kinetic EDB.

for all values of *n* and κ because AS is a nonabsorbing aerosol and purely scattering (Figure 3a). For κ values below 0.4, the RFE is insensitive to *n*. Then, as hygroscopicity increases, the RFE takes values that are less negative and shows more dependency on *n* for this particle size. An uncertainty of ±0.1 in κ translates into a ΔRFE of ~ ±1% at 90% RH (Figure 3b). At 99% RH, this uncertainty in κ translates into a ΔRFE of ~ ±3% (Figure 3d). Overall, the range in RFE (ΔRFE) is less than ±7% for typical uncertainty in *n* of ±0.02, derived from ensemble BB-CRDS measurements, and uncertainties in κ under high RHs ($0.33 < \kappa < 0.7$). This is consistent with the results provided by Zarzana et al. (2014), who considered AS under only dry conditions. Therefore, an increase in RH does not imply an increase in the uncertainty in the evaluated RFE in the range of values considered of *n* and κ for AS aerosol in the atmospheric relevant size of 0.1 μm. The range in RFE (ΔRFE) estimated is reduced to values ~ ±1% (red box) when we consider typical uncertainties achieved by more refined measurements of *n* (±0.003) from BB-CRDS and uncertainties of κ (±0.01) using a CK-EDB. Such refined measurements are not important for particles of this size range.

For typical AS sizes with the largest RF in the atmosphere (dry particle radius of 0.35 μm; Zhuang et al., 1999), the range in RFE (ΔRFE) increases to ±20% at 90% RH when the maximum uncertainties in the *n* and κ are considered (Figures 4a and 4b) from conventional measurements. The range in RFE decreases to ±15% at 99% RH with pronounced oscillations in RFE due to the appearance of Mie resonance structure at the wet particle sizes to which the dry particle has grown (Figure 4c). The range of RFE (ΔRFE) is considerably reduced to values ~ ±5% (red box) once the refined accuracies of measurements of *n* and κ from BB-CRDS and CK-EDB measurements, respectively, are considered (Figure 4d). For particles of this size, improved measurements of *n* and κ could lead to improvements in estimations of RFE.

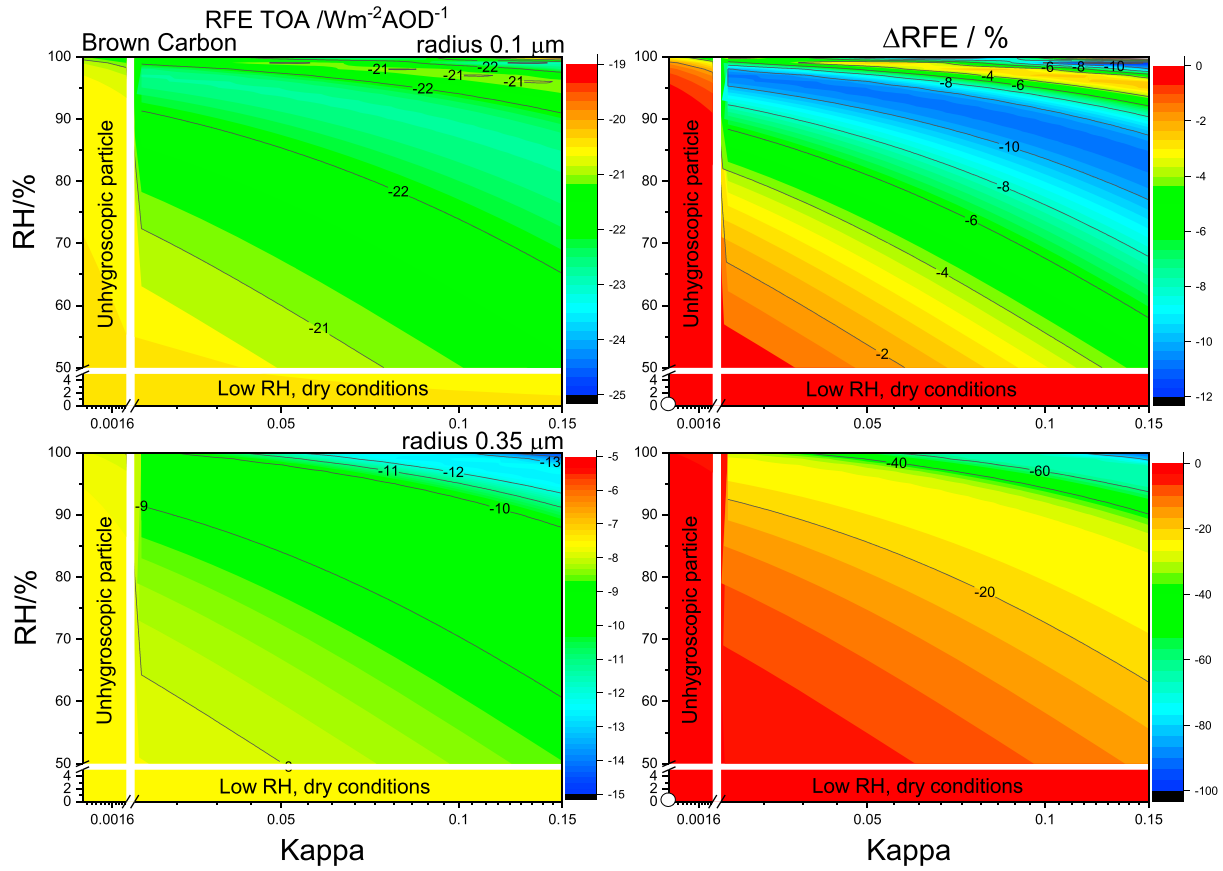

Figure 5. Contour plots representing (a) the RFE and (b) ΔRFE as function of κ and RH for BrC particles of dry radius 0.1 μm (the white dot means reference value for *n* and κ). (c and d) Same as (a) and (b) but for particles of dry radius 0.35 μm.

In summary, for dry particle radius of 0.1 μm at low κ values, the RFE does not depend on *n*, but when the hygroscopicity increases, the dependency of the RFE on *n* is not negligible. The range of the RFE (ΔRFE) from the uncertainties of *n* and κ associated with typical measurements is less than ±7%, and it is not affected by an increase of RH. If we consider typical sizes of AS in the atmosphere (0.35 μm), the range of the RFE (ΔRFE) increases to ±20% at 90% RH and ±15% at 99% RH for the typical uncertainties associated with *n* and κ. The uncertainties in radiative effects are considerably reduced to typically ~ ±5% once the refined accuracies of measurements of *n* and κ from BB-CRDS and CK-EDB measurements for AS dry particle radius of 0.35 μm, respectively, are considered. We have limited our comparisons here to only two particle sizes, two RHs, and one wavelength; similar comparisons result when considering the full range of these variables.

3.3. Sensitivity of the RFE to Refractive Index and Hygroscopic κ-Factor for Absorbing Aerosol

We next consider the impact of uncertainties in the hygroscopic growth on the RH-dependent RFE of BrC aerosol. To our knowledge, this represents the first assessment of the impact of κ on light absorption by BrC. We take the work of Zarzana et al. (2014), who report values of *n* and *k* of 1.65 and 0.05 for BrC aerosol particles under dry conditions, as a reference refractive index. When RH increases, the *n* and *k* values of the refractive index are scaled using equations given by Hänel (1976) as discussed in section 2.3.

Figures 5a and 5b show RFE and the ΔRFE, respectively, as functions of RH and κ, ranging from low RHs to saturated conditions for BrC particles of 0.1 μm dry radius. Unlike the pure scattering AS particles, the RFE for BrC particles takes more negative values as the RH increases above 50% RH due to the particle size change, although there is some nonmonotonic behavior. As would be expected, this trend depends on the value of κ (Figure 5a). Although *g* rises for higher RHs and κ values (figure not shown) increasing the scattered light in forward direction, the higher values of κ lead to smaller values of absorption due to dilution of

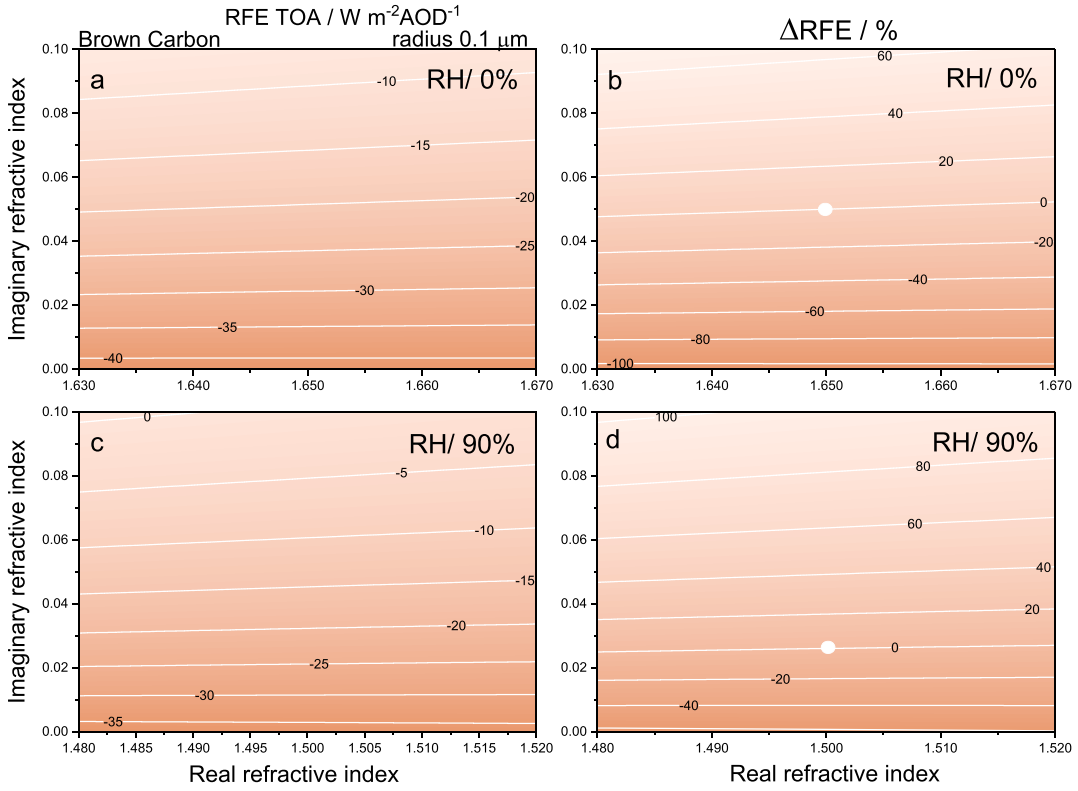

Figure 6. Contour plots representing (a) RFE and (b) ΔRFE as function of *n* and *k* for BrC particles of dry radius 0.1 μm at 532 nm wavelength and dry conditions (the white dot means reference value for *n* and κ). (c and d) Same as (a) and (b) but for 90% RH. The full ranges in *n* and *k* represent the typical uncertainty ranges in these values from conventional approaches.

the *k* and, hence, the ω reaches higher values. As a result, an increase of the β to space, and hence cooling at the top of the atmosphere, occurs. The ΔRFE for RHs ~100% relative to dry conditions for BrC aerosol (the white dot, bottom left corner of plot, the usual conditions considered by previous studies) reaches −12% value, showing that the hygroscopic effect should not be neglected in radiative effects (Figure 5b).

For larger BrC particle size (0.35 μm dry radius), there is less cooling compared to smaller particles at the top of the atmosphere under dry and low RH conditions (Figure 5c). At RH >50%, the hygroscopic growth increases and an increase in RH and κ leads to a large change in RFE and an enhancement in the cooling effect. The hygroscopic growth leads to a significant decrease in the imaginary part of the refractive index, leading to a smaller impact of absorption, an effect which is discussed further below. The ΔRFE for RHs ~100% compared to dry conditions (white dot) can take values as large as −100% if the hygroscopic growth is at the upper end of estimates (Figure 5d).

To provide an example of the impact of the uncertainties in RFE presented here on the RF, we assume an aerosol concentration for the BrC aerosol based on the tabulated characteristics of the water-soluble organic aerosol component given by Hess et al. (1998). For average continental aerosol, we consider an aerosol concentration of 7,000 cm^{-3} (Hess et al., 1998, Table 4). Assuming a 1-km aerosol layer height, the AOD at 532 nm wavelength for the average continental BrC aerosol is around 0.02 at an RH of 0% and around 0.06 at RHs higher than 80%. Indeed, for BrC aerosol with particle dry radius of 0.1 and 0.35 μm, the difference between cases with values of κ of 0.15 and 0 is equal to a difference of about −0.42 and −0.72 W/m^2, respectively, in RF. Considering that the estimated overall climate forcing of anthropogenic aerosol particles is of the order of −1 W/m^2, an accurate determination of κ is crucial to constrain more precise RF values. Our findings agree well with those for organic aerosol provided by Rastak et al. (2017).

The sensitivity of the RFE to uncertainties in *n* and *k* along with hygroscopic effects (RH and κ) with respect to chosen reference values is now assessed. Again, we take the refractive index values given by Zarzana et al.

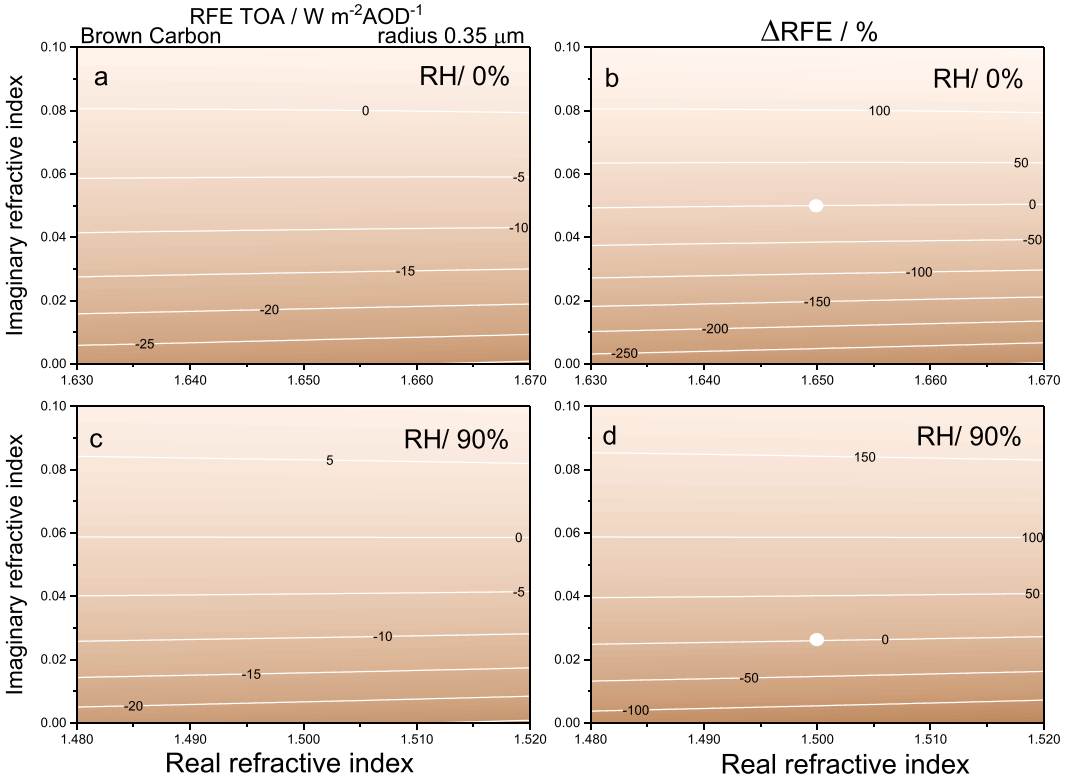

Figure 7. Contour plots representing (a) RFE and (b) ΔRFE as function of *n* and *k* for BrC particles of dry radius 0.35 μm at 532 nm wavelength and dry conditions (the white dot means reference value for *n* and κ). (c and d) Same as (a) and (b) but for 90% RH.

(2014) for *n* and *k* (1.65 and 0.05, respectively) for BrC aerosol under dry conditions as the reference case. We assume a κ of 0.1, a typical indicative mean value for hygroscopic growth of aged organic aerosol. We assume the dependence of *n* and *k* on RH given by equations (10) and (11). Uncertainties of *n* and *k* for BrC retrieved by Zarzana et al. (2014) from CRDS measurements for ensembles of particles are used to explore the sensitivity to refractive index.

For particles of 0.1 μm dry radius, an uncertainty of ±0.01 in *k* causes a ΔRFE around ±20% (Figures 6a and 6b). Zarzana et al. (2014) estimated similar sensitivity when evaluating the uncertainty for BrC particles of 0.075 μm radius under dry conditions. Indeed, a similar range of the RFE values (ΔRFE) is found when considering the same uncertainty in *k* at 90% RH (Figures 6c and 6d). Therefore, the hygroscopicity of the particles does not change the uncertainty in the RFE modeled for particles of dry radius 0.1 μm. Similarly, for particles of 0.35 μm dry radius, an uncertainty of ±0.01 in *k* causes a range of the RFE values (ΔRFE) around ±50% under dry conditions (Figures 7a and 7b). As RH is increased to 90%, the range of the RFE values (ΔRFE) is similar to dry conditions (Figures 7c and 7d). Therefore, for this size of BrC particle, the precision on *k* must be below ±0.001 if we want to reduce uncertainties in RFE below ±5%. The sensitivity the RFE to the *n* at all RHs is rather weak.

In summary, small BrC particles (0.1 μm) cause cooling at the top of the atmosphere, and as the RH and κ increase, the RFE is more negative compared to the usual assumptions of dry unhygroscopic BrC. This suggests that the hygroscopic growth of BrC should not be neglected in estimating radiative effects although it contributes a smaller uncertainty than the current uncertainty in the value of *k*. For larger BrC particles (0.35 μm), there is less cooling at the top of the atmosphere under dry and low RH conditions. However, at higher RHs >50% and for more hygroscopic particles, the hygroscopic growth leads to a large change in RFE and an enhancement in the cooling effect. The ΔRFE for RHs ~100% compared to dry conditions can take values around −100% (Figure 5d). On the other hand, the impact of the uncertainty on *k* over the range of values of the RFE (ΔRFE) is unaffected by the uncertainty in the hygroscopicity. However, the range of

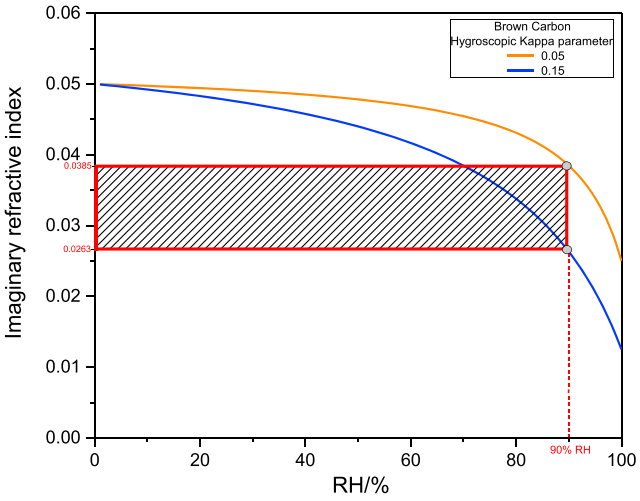

Figure 8. Imaginary refractive index as a function of RH at two values of κ (0.05 and 0.15) for BrC.

values of the RFE (ΔRFE) is strongly increased over the full range of uncertainty of *k* when the size of BrC particles increases.

Up to this point we have assumed a constant value of κ in order to evaluate the sensitivity of the RFE to real and imaginary refractive indices. As is apparent from Figures 6 and 7, the dependency of the RFE is strong on *k* and weak on *n*. However, we now evaluate the interdependency of the *k* and κ on the RH, taking into account the range of reported values of κ for BrC. Figure 8 shows the estimated change of *k* with RH for typically expected upper and lower values of κ. At low RHs, *k* is not sensitive to κ. However, *k* is increasingly affected by the value of κ as the RH increases. At 90% RH, an increase in the value of κ from 0.05 to 0.15 reduces the value of *k* from 0.0385 to 0.0263. Thus, an uncertainty of 0.1 in κ is translated to an uncertainty of 0.0122 in *k* at this RH. The increase in hygroscopicity leads to increasing dilution of the absorbing components in the BrC aerosol and a reduction in the *k*. This will have implications from point of view of radiative effects.

The range of RFE for BrC particles for realistic ranges of *k* and κ is evaluated and reported at 90% RH in Figure 9. The scale used in the axis of κ contains values from unhygroscopic aerosol (κ equal to zero) to the largest potential values for BrC particles (κ equal to 0.15). For smaller particles (0.1 μm of dry radius), the RFE takes values in the range from −40 to $-10\ \mathrm{W \cdot m^{-2} \cdot AOD^{-1}}$ (Figure 9a). It is slightly sensitive to κ and strongly sensitive to *k*. As evaluated above, the range of values for *k* is between 0.0385 and 0.0263 at 90% RH. In this sense, the range of the RFE (ΔRFE) compared to dry conditions (equivalent to placing a white dot on the mean value of *k* and a κ value of 0 as

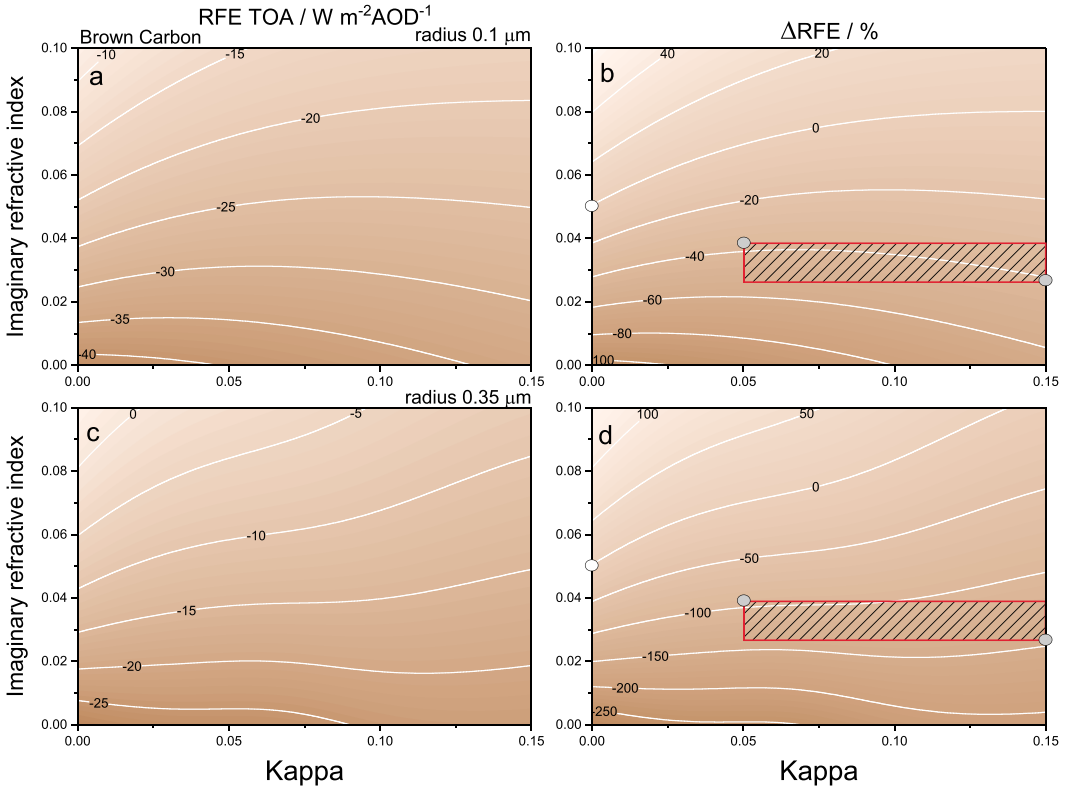

Figure 9. Contour plots representing (a) RFE and (b) ΔRFE as function of *k* and κ for BrC particles of dry radius 0.1 μm at 90% RH (the white dot means RFE at dry conditions). (c and d) Same as (a) and (b) but for BrC particles of dry radius 0.35 μm. The full ranges in *n* and κ represent the typical uncertainty ranges in these values from conventional approaches.

Table 1
Precision in the Top of the Atmosphere of the Radiative Forcing Efficiency Considering Uncertainties n, k, and κ at Different Relative Humidities for 0.1 and 0.35 μm Dry Radius AS and BrC Particles

		Precision in the radiative forcing efficiency at the top of the atmosphere								
		Ammonium Sulfate				Brown carbon				
Dry radius (μm)	RH	Uncertainty in *n* from CRDS (±0.02)	Uncertainty in κ from HTDM (0.33–0.72)	Uncertainty in *n* from BB-CRDS (±0.003)	Uncertainty in κ from CK-EDB (±0.01)	Uncertainty in *n* from CRDS (±0.02)	Uncertainty in *k* (±0.01)	Assumed value of κ (0.1)	Uncertainty in *k* (±0.0122)	Uncertainty in κ (0.05–0.15)
0.1	Dry conditions	-		-			±20%		-	
	90%	±5–7%		±1%			±20%		±20%	
	99%	±5–7%		±1%			-		-	
0.35	Dry conditions	-		-			±50%		-	
	90%	±20%		±5%			±50%		±55%	
	99%	±15%		±5%			-		-	

indicated) is between −35 and −55% (the red box indicates the uncertainty of RFE due to the uncertainty in *k*; Figure 9b). The negative sign indicates that radiative impact of BrC particles at 90% RH is shifted toward a cooling of the atmosphere relative to the dry conditions. In the case of larger BrC particles (0.35 μm of dry radius) the RFE takes less negative values and can even imply a warming of the atmosphere at high *k* (Figure 9c). However, the range of RFE (ΔRFE) estimates relative to dry conditions is higher than for smaller particles (from −85 to −140%; the red box indicates uncertainty of RFE due to the uncertainty in *k*; Figure 9d). Consistent with this analysis, it is important to calculate more precise values of *k* as a function of RH while incorporating the uncertainty in κ. Indeed, reducing the uncertainty in κ for BrC aerosol is important: the uncertainty in the RFE may be up to −140% relative to dry conditions for particles of 0.35 μm of dry radius.

4. Conclusions

So far, the accuracy of the aerosol refractive index under dry conditions has been the key quantity considered in an assessment of the direct RF. Studies that consider the RH dependence estimate the water-soluble aerosol refractive index through the conventional volume mixing rule. However, significant differences in the RF values are expected based on refined empirical refractive index retrieved from single-particle BB-CRDS measurements. Less attention has been paid in evaluating the influence of uncertainties in the hygroscopic kappa parameter on the RF. According with our analysis the dominance of this parameter may be a significant factor even more important than the refractive index values in some cases. Its influence depends on the aerosol type (nonabsorbing and absorbing particles) and on the particle size. Larger differences in the RFE for absorbing particles are found when RH, hygroscopic kappa parameter, and particle size increase compared to dry conditions. Further, the precision of the RFE with the imaginary refractive index depends on the size of the BrC particle. Therefore, our results suggest that uncertainties in the hygroscopic kappa parameter should be incorporated in the estimated uncertainty in RF by AS and BrC aerosol.

The specific contributions of this study can now be summarized. First, we implement a more precise data set of refractive indices for nonabsorbing aerosol than previously used in other studies, retrieved from BB-CRDS measurements of single particles. There are a few studies that scale the aerosol optical properties with the RH (Kiehl et al., 2000; Li et al., 2001). However, the refractive indices used in these studies were retrieved from volume-weighted averages of refractive indices. Erlick et al. (2011) reported that the difference between the conventional volume mixing rule and empirically derived refractive indices may be important as radiative effects are evaluated. We demonstrate that it is possible to provide more accurate RFE values using refined optical properties (precise refractive indices) and microphysical properties (single sizes) from BB-CRDS measurements. Second, as far as we know, we consider for the first time the sensitivity of the RFE to uncertainties in the complex refractive index and the hygroscopic kappa parameter from dry conditions up to saturated conditions. Third, the study of the sensitivity of RFE is extended to absorbing aerosols. BrC aerosol is considered, and the radiative effects as a function of the complex refractive index and hygroscopic kappa parameter are evaluated based on *n*, *k*, and κ values from literature. Table 1

summarizes the estimated accuracies of RFE estimates arising from uncertainties of n, k, and κ at different RHs and for two different sizes of AS and BrC particles.

As future lines of work, we are moving toward measurements on nonspherical scatterers using a new experimental approach with a combination of an electrodynamic linear quadrupole trap and a cavity ring down spectrometer. We will examine in a later manuscript the uncertainties in optical and physical properties in different environmental conditions for these types of particles and their potential radiative impact.

Acknowledgments
Antonio Valenzuela thanks the European Union's Horizon 2020 research and innovation program through grant MSCA-IF-EF-ST (grant agreement 700843). Bryan R. Bzdek acknowledges support from the Natural Environment Research Council (NERC) through grant NE/P018459/1. The data used are listed at https://doi.org/10.5523/bris.30gtnejo25luq21rqwo94yeru6.

References

Adams, P. J., Seinfeld, J. H., Koch, D., Mickley, L., & Jacob, D. (2001). General circulation model assessment of direct radiative forcing by the sulfate-nitrate-ammonium-water inorganic aerosol system. *Journal of Geophysical Research*, *106*, 1097–1111. https://doi.org/10.1029/2000JD900512

Boucher, O. (1998). On aerosol direct shortwave forcing and the Henyey-Greenstein phase function. *Journal of the Atmospheric Sciences*, *55*(1), 128–134. https://doi.org/10.1175/1520-0469(1998)055%3C0128:OADSFA%3E2.0.CO;2

Boucher, O., & Lohmann, U. (1995). The sulfate-CCN-cloud albedo effect: A sensitivity study with two general circulation models. *Tellus Series B*, *47*, 281–300.

Charlson, R. J., Covert, D. S., Larson, T. V., & Waggoner, A. P. (1978). Chemical properties of tropospheric sulfur aerosols. *Atmospheric Environment*, *12*(1-3), 39–53. https://doi.org/10.1016/0004-6981(78)90187-7

Charlson, R. J., Schwartz, S. E., Hales, J. M., Cess, R. D., Coakley, J. A., Hansen, J. E., & Hofmann, D. J. (1992). Climate forcing by anthropogenic aerosols. *Science*, *255*(5043), 423–430. https://doi.org/10.1126/science.255.5043.423

Chen, Y., & Bond, T. C. (2010). Light absorption by organic carbon from wood combustion. *Atmospheric Chemistry and Physics*, *10*(4), 1773–1787. https://doi.org/10.5194/acp-10-1773-2010

Colberg, C. A., Luo, B. P., Wernli, H., Koop, T., & Peter, T. (2003). A novel model to predict the physical state of atmospheric $H_2SO_4/NH_3/H_2O$ aerosol particles. *Atmospheric Chemistry and Physics*, *3*(4), 909–924. https://doi.org/10.5194/acp-3-909-2003

Cotterell, M. I., Mason, B. J., Preston, T. C., Orr-Ewing, A. J., & Reid, J. P. (2015). Optical extinction efficiency measurements on fine and accumulation mode aerosol using single particle cavity ring-down spectroscopy. *Physical Chemistry Chemical Physics*. https://doi.org/10.1039/C5CP00252D

Cotterell, M. I., Preston, T. C., Mason, B. J., Orr-Ewing, A. J., & Reid, J. P. (2015). Extinction cross section measurements for a single optically trapped particle. *Proceedings of SPIE*, *9548* (11 pp.). https://doi.org/10.1117/12.2189174

Cotterell, M. I., Preston, T. C., Orr-Ewing, A. J., & Reid, J. P. (2016). Assessing the accuracy of complex refractive index retrievals from single aerosol particle cavity ring-down spectroscopy. *Aerosol Science and Technology*, *50*(10), 1077–1095. https://doi.org/10.1080/02786826.2016.1219691

Cotterell, M. I., Willoughby, R. E., Bzdek, B. R., Orr-Ewing, A. J., & Reid, J. P. (2017). A complete parameterization of the relative humidity and wavelength dependence of the refractive index of hygroscopic inorganic aerosol particles. *Atmospheric Chemistry and Physics*, *17*(16), 9837–9851. https://doi.org/10.5194/acp-17-9837-2017

D'Almeida, G. A., Koepke, P., & Shettle, E. P. (1991). *Atmospheric aerosols: Global climatology and radiative characteristics*. Hampton, VA: A. Deepak Pub.

Dinar, E., Riziq, A. A., Spindler, C., Erlick, C., Kiss, G., & Rudich, Y. (2008). The complex refractive index of atmospheric and model humic-like substances (HULIS) retrieved by a cavity ring down aerosol spectrometer (CRD-AS). *Faraday Discussions*, *137*, 279–295. https://doi.org/10.1039/b703111d

Duplissy, J., DeCarlo, P. F., Dommen, J., Alfarra, M. R., Metzger, A., Barmpadimos, I., et al. (2011). Relating hygroscopicity and composition of organic aerosol particulate matter. *Atmospheric Chemistry and Physics*, *11*(3), 1155–1165. https://doi.org/10.5194/acp-11-1155-2011

Erlick, C., Abbatt, J. P., & Rudich, Y. (2011). How different calculations of the refractive index affect estimates of the radiative forcing efficiency of ammonium sulfate aerosols. *Journal of the Atmospheric Sciences*, *68*(9), 1845–1852. https://doi.org/10.1175/2011JAS3721.1

Erlick, C., & Frederick, J. E. (1998). Effects of aerosols on the wavelength dependence of atmospheric transmission in the ultraviolet and visible: 2. Continental and urban aerosols in clear skies. *Journal of Geophysical Research*, *103*, 23,275–23,285.

Fitzgerald, J. W. (1975). Approximation formulas for the equilibrium size of an aerosol particle as a function of its dry size and composition and the ambient relative humidity. *Journal of Applied Meteorology*, *14*(6), 1044–1049. https://doi.org/10.1175/1520-0450(1975)014%3C1044:AFFTES%3E2.0.CO;2

Flores, J. M., Bar-Or, R. Z., Bluvshtein, N., Abo-Riziq, A., Kostinski, A., Borrmann, S., et al. (2012). Absorbing aerosols at high relative humidity: Linking hygroscopic growth to optical properties. *Atmospheric Chemistry and Physics*, *12*(12), 5511–5521. https://doi.org/10.5194/acp-12-5511-2012

Garland, J. A. (1969). Condensation on ammonium sulphate particles and its effect on visibility. *Atmospheric Environment*, *3*(3), 347–354. https://doi.org/10.1016/0004-6981(69)90108-5

Good, N., Topping, D. O., Duplissy, J., Gysel, M., Meyer, N. K., Metzger, A., et al. (2010). Widening the gap between measurement and modelling of secondary organic aerosol properties? *Atmospheric Chemistry and Physics*, *10*(6), 2577–2593. https://doi.org/10.5194/acp-10-2577-2010

Hänel, G. (1976). The properties of atmospheric aerosol particles as functions of the relative humidity at thermodynamic equilibrium with the surrounding moist air. *Advances in Geophysics*, *19*, 73–188. https://doi.org/10.1016/S0065-2687(08)60142-9

Haywood, J., & Boucher, O. (2000). Estimates of the direct and indirect radiative forcing due to tropospheric aerosols: A review. *Reviews of Geophysics*, *38*, 513–543. https://doi.org/10.1029/1999RG000078

Haywood, J. M., Roberts, D. L., Slingo, A., Edwards, J. M., & Shine, K. P. (1997). General circulation model calculations of the direct radiative forcing by anthropogenic sulphate and fossil-fuel soot aerosol. *Journal of Climate*, *10*(7), 1562–1577. https://doi.org/10.1175/1520-0442(1997)010%3C1562:GCMCOT%3E2.0.CO;2

Haywood, J. M., & Shine, K. P. (1995). The effect of anthropogenic sulfate and soot aerosol on the clear sky planetary radiation budget. *Geophysical Research Letters*, *22*, 603–606. https://doi.org/10.1029/95GL00075

Heald, C. L., Ridley, D. A., Kroll, J. H., Barrett, S. R. H., Cady-Pereira, K. E., Alvarado, M. J., & Holmes, C. D. (2014). Contrasting the direct radiative effect and direct radiative forcing of aerosols. *Atmospheric Chemistry and Physics*, *14*. https://doi.org/10.5194/acp-14-5513-2014(11), 5513–5527.

Hess, M., Koepke, P., & Schult, I. (1998). Optical properties of aerosols and clouds: The software package OPAC. *Bulletin of the American Meteorological Society*, *79*(5), 831–844. https://doi.org/10.1175/1520-0477(1998)079%3C0831:OPOAAC%3E2.0.CO;2

Intergovernmental Panel on Climate Change (2013). Annex V: Contributors to the IPCC WGI Fifth Assessment Report. In T. F. Stocker, et al. (Eds.), *Climate Change 2013: The Physical Science Basis. Contribution of Working Group I to the Fifth Assessment Report of the Intergovernmental Panel on Climate Change*. Cambridge, United Kingdom and New York, NY: Cambridge University Press.

Kiehl, J. T., Schneider, T. L., Rasch, P. J., Barth, M. C., & Wong, J. (2000). Radiative forcing due to sulfate aerosols from simulations with the National Center for Atmospheric Research Community Climate, Version 3. *Journal of Geophysical Research*, *105*, 1441–1457. https://doi.org/10.1029/1999JD900495

Kirkevåg, A., Iversen, T., Seland, Ø., Hoose, C., Kristjánsson, J. E., Struthers, H., et al. (2013). Aerosol–climate interactions in the Norwegian Earth System Model – NorESM1-M. *Geoscientific Model Development*, *6*(1), 207–244. https://doi.org/10.5194/gmd-6-207-2013

Koehler, K. A., Kreidenweis, S. M., DeMott, P. J., Prenni, A. J., Carrico, C. M., Ervens, B., & Feingold, G. (2006). Water activity and activation diameters from hygroscopicity data—Part II: Application to organic species. *Atmospheric Chemistry and Physics*, *6*(3), 795–809. https://doi.org/10.5194/acp-6-795-2006

Kreidenweis, S. M., Koehler, K., DeMott, P. J., Prenni, A. J., Carrico, C., & Ervens, B. (2005). Water activity and activation diameters from hygroscopicity data—Part I: Theory and application to inorganic salts. *Atmospheric Chemistry and Physics*, *5*(5), 1357–1370. https://doi.org/10.5194/acp-5-1357-2005

Li, J., Wong, J. G. D., Dobbie, J. S., & Chylek, P. (2001). Parameterization of the optical properties and growth of sulfate aerosols. *Journal of the Atmospheric Sciences*, *58*(2), 193–209. https://doi.org/10.1175/1520-0469(2001)058%3C0193:POTOPO%3E2.0.CO;2

Marsh, A., Rovelli, G., Song, Y.-C., Pereira, K. L., Willoughby, R. E., Bzdek, B. R., et al. (2017). Accurate representations of the physicochemical properties of atmospheric aerosols: When are laboratory measurements of value? Faraday discuss. [internet]. *Royal Society of Chemistry*, *200*, 639–661.

Mason, B. J., Cotterell, M. I., Preston, T. C., Orr-Ewing, A. J., & Reid, J. P. (2015). Direct measurements of the optical cross sections and refractive indices of individual volatile and hygroscopic aerosol particles. *The Journal of Physical Chemistry. A*, *119*(22), 5701–5713. https://doi.org/10.1021/acs.jpca.5b00435

Mason, B. J., King, S.-J., Miles, R. E. H., Manfred, K. M., Rickards, A. M. J., Kim, J., et al. (2012). Comparison of the accuracy of aerosol refractive index measurements from single particle and ensemble techniques. *Journal of Physical Chemistry. A*, *116*, 8547–8556. https://doi.org/10.1021/jp3049668

McCartney, E. J. (1976). *Optics of the atmosphere—Scattering by molecules and particles*. New York: John Wiley.

Miles, R. E. H., Carruthers, A. E., & Reid, J. P. (2011). Novel optical techniques for measurements of light extinction, scattering and absorption by single aerosol particles. *Laser & Photonics Reviews*, *5*(4), 534–552. https://doi.org/10.1002/lpor.201000029

Myhre, G., Samset, B. H., Schulz, M., Balkanski, Y., Bauer, S., Berntsen, T. K., et al. (2013). Radiative forcing of the direct aerosol effect from AeroCom Phase II simulations. *Atmospheric Chemistry and Physics*, *13*(4), 1853–1877. https://doi.org/10.5194/acp-13-1853-2013

Myhre, G., Stordal, F., Berglen, T. F., Sundet, J. K., & Isaksen, I. S. A. (2004). Uncertainties in the radiative forcing due to sulphate aerosols. *Journal of the Atmospheric Sciences*, *61*(5), 485–498. https://doi.org/10.1175/1520-0469(2004)061%3C0485:UITRFD%3E2.0.CO;2

Nemesure, S., Wagener, R., & Schwartz, S. E. (1995). Direct shortwave forcing of climate by anthropogenic sulfate aerosol: Sensitivity to particle size, composition, and relative humidity. *Journal of Geophysical Research*, *100*, 26,105–26,116. https://doi.org/10.1029/95JD02897

Penner, J. E., Charlson, R. J., Hales, J. M., Laulainen, N. S., Leifer, R., Novakov, T., et al. (1994). Quantifying and minimizing uncertainty of climate forcing by anthropogenic aerosols. *Bulletin of the American Meteorological Society*, *75*(3), 375–400. https://doi.org/10.1175/1520-0477(1994)075%3C0375:QAMUOC%3E2.0.CO;2

Petters, M. D., & Kreidenweis, S. M. (2007). A single parameter representation of hygroscopic growth and cloud condensation nucleus activity. *Atmospheric Chemistry and Physics*, *7*(8), 1961–1971. https://doi.org/10.5194/acp-7-1961-2007

Pilinis, C., Pandis, S. N., & Seinfeld, J. H. (1995). Sensitivity of direct climate forcing by atmospheric aerosols to aerosol size and composition. *Journal of Geophysical Research*, *100*, 18,739–18,754. https://doi.org/10.1029/95JD02119

Randles, C. A., Russell, L. M., & Ramaswamy, V. (2004). Hygroscopic and optical properties of organic sea salt aerosol and consequences for climate forcing. *Geophysical Research Letters*, *31*, L16108. https://doi.org/10.1029/2004GL020628

Rastak, N., Pajunoja, A., Acosta Navarro, J. C., Ma, J., Song, M., Partridge, D. G., et al. (2017). Microphysical explanation of the RH-dependent water affinity of biogenic organic aerosol and its importance for climate. *Geophysical Research Letters*, *44*, 5167–5177. https://doi.org/10.1002/2017GL073056

Rovelli, G., Miles, R. E. H., Reid, J. P., & Clegg, S. L. (2016). Accurate measurements of aerosol hygroscopic growth over a wide range in relative humidity. *The Journal of Physical Chemistry. A*, *120*(25), 4376–4388. https://doi.org/10.1021/acs.jpca.6b04194

Sellmeier, W. (1871). Zur Erklärung der abnormen Farbenfolge im Spektrum einiger Substanzen. *Annals of Physics*, *143*, 272–282.

Stocker, T. F., Qin, D., Plattner, G.-K., Tignor, M., Allen, S. K., Boschung, J., et al. (2013). IPCC, 2013: Climate Change 2013: The Physical Science Basis. Contribution of Working Group I to the Fifth Assessment Report of the Intergovernmental Panel on Climate Change. In T. F. Stocker, et al. (Eds.) (pp. 33–116). Cambridge, UK: Cambridge University Press.

Sutton, L. E., & Stavroudis, O. N. (1961). Fitting refractive index data by least squares. *Journal of the Optical Society of America*, *51*(8), 901. https://doi.org/10.1364/JOSA.51.000901

Tang, I. N. (1996). The chemical and size effects of hygroscopic aerosols on light scattering coefficients. *Journal of Geophysical Research*, *101*, 19,245–19,250.

Tang, I. N., & Munkelwitz, H. R. (1994). Water activities, densities, and refractive indices of aqueous sulfate and nitrate droplets of atmospheric importance. *Journal of Geophysical Research*, *99*, 18,801–18,808.

Tang, I. N., Tridico, A. C., & Fung, K. H. (1997). Thermodynamic and optical properties of sea salt aerosols. *Journal of Geophysical Research*, *102*, 23,269–23,275. https://doi.org/10.1029/97JD01806

Tatian, B. (1964). Interpolation of glass indices with applications to first order axial chromatic aberration, Itek Corp. Report OR-63-20, Lexington, Mass.

Tatian, B. (1984). Fitting refractive-index data with the Sellmeier dispersion formula. *Applied Optics*, *23*(24), 4477–4485. https://doi.org/10.1364/AO.23.004477

Taylor, N. F., Collins, D. R., Lowenthal, D. H., McCubbin, I. B., Hallar, A. G., Samburova, V., et al. (2017). Hygroscopic growth of water soluble organic carbon isolated from atmospheric aerosol collected at US national parks and Storm Peak Laboratory. *Atmospheric Chemistry and Physics*, *17*, 2555–2571. https://doi.org/10.5194/acp-17-2555-2017

Titos, G., Cazorla, A., Zieger, P., Andrews, E., Lyamani, H., Granados-Muñoz, M. J., et al. (2016). Effect of hygroscopic growth on the aerosol light-scattering coefficient: A review of measurements, techniques and error sources. *Atmospheric Environment*, *141*, 494–507. https://doi.org/10.1016/j.atmosenv.2016.07.021

van de Hulst, H. C. (1957). *Light scattering by small particles*. New York: John Wiley.

Walker, J. S., Carruthers, A. E., Orr-Ewing, A. J., & Reid, J. P. (2013). Measurements of light extinction by single aerosol particles. *Journal of Physical Chemistry Letters*, *4*(10), 1748–1752. https://doi.org/10.1021/jz4008068

Wang, J., Jacob, D. J., & Martin, S. T. (2008). Sensitivity of sulfate direct climate forcing to the hysteresis of particle phase transitions. *Journal of Geophysical Research*, *113*, D11207. https://doi.org/10.1029/2007JD009368

Willoughby, R. E., Cotterell, M. I., Lin, H., Orr-Ewing, A. J., & Reid, J. P. (2017). Measurements of the imaginary component of the refractive index of weakly absorbing single aerosol particles. *Journal of Physical Chemistry*, *121*(30), 5700–5710.

Wiscombe, W. J., & Grams, G. W. (1976). The backscattered fraction in two-stream approximations. *Journal of the Atmospheric Sciences*, *33*(12), 2440–2451. https://doi.org/10.1175/1520-0469(1976)033%3C2440:TBFITS%3E2.0.CO;2

Zarzana, K. J., Cappa, C. D., & Tolbert, M. A. (2014). Sensitivity of aerosol refractive index retrievals using optical spectroscopy. *Aerosol Science and Technology*, *48*(11), 1133–1144. https://doi.org/10.1080/02786826.2014.963498

Zhang, K., O'Donnell, D., Kazil, J., Stier, P., Kinne, S., Lohmann, U., et al. (2012). The global aerosol-climate model ECHAM-HAM, version 2: Sensitivity to improvements in process representations. *Atmospheric Chemistry and Physics*, *12*(19), 8911–8949. https://doi.org/10.5194/acp-12-8911-2012

Zhuang, H., Chan, C. K., Fang, M., & Wexler, A. S. (1999). Size distributions of particulate sulfate, nitrate, and ammonium at a coastal site in Hong Kong. *Atmospheric Environment*, *33*(6), 843–853. https://doi.org/10.1016/S1352-2310(98)00305-7

Zieger, P., Fierz-Schmidhauser, R., Gysel, M., Strom, J., Henne, S., Yttri, K. E., et al. (2010). Effects of relative humidity on aerosol light scattering in the Arctic. *Atmospheric Chemistry and Physics*, *10*(8), 3875–3890. https://doi.org/10.5194/acp-10-3875-2010